Chinese Journal of Chemistry, **2006**, *24*, 887—893

Full Paper

Theoretical Study on N—H···O Blue-shifted H-Bond for $HNO\cdots H_2O_2$ Complex

YANG, Yong*(杨颙) ZHANG, Wei-Jun(张为俊) GAO, Xiao-Ming(高晓明)

Environmental Spectroscopy Laboratory, Anhui Institute of Optics and Fine Mechanics, Chinese Academy of Sciences, Hefei, Anhui 230031, China

A theoretical study on the blue-shifted H-bond N—H···O and red-shifted H-bond O—H···O in the complex $HNO\cdots H_2O_2$ was conducted by employment of both standard and counterpoise-corrected methods to calculate the geometric structures and vibrational frequencies at the MP2/6-31G(d), MP2/6-31+G(d,p), MP2/6-311++G(d,p), B3LYP/6-31G(d), B3LYP/6-31+G(d,p) and B3LYP/6-311++G(d,p) levels. In the H-bond N—H···O, the calculated blue shift of N—H stretching frequency is in the vicinity of 120 cm^{-1} and this is indeed the largest theoretical estimate of a blue shift in the X—H···Y H-bond ever reported in the literature. From the natural bond orbital analysis, the red-shifted H-bond O—H···O can be explained on the basis of the dominant role of the hyperconjugation. For the blue-shifted H-bond N—H···O, the hyperconjugation was inhibited due to the existence of significant electron density redistribution effect, and the large blue shift of the N—H stretching frequency was prominently due to the rehybridization of sp^n N—H hybrid orbital.

Keywords red-shifted H-bond, blue-shifted H-bond, atoms in molecules topological analysis, natural bond orbital analysis

Introduction

The unusual phenomenon of blue-shifted or improper X—H···Y H-bond accompanied by X—H bond contraction and a blue shift of the X—H bond stretching frequency continues to receive significant experimental and theoretical attention.[1-32] The blue-shifted H-bonds that have been extensively studied so far are mainly C—H···Y systems. However, blue-shifted H-bonds N—H···Y are very interesting since N atom is more electronegative than C atom and N—H bond is a better proton donor than C—H bond. Both Hobza and Li *et al*.[7,23] have predicted a blue-shifted or improper N—H···F H-bond existing in $NHF_2\cdots HF$ complex at MP2/6-31G(d,p) and MP2/6-311+G(d,p). Unexpectedly, Lu and coworkers[28] have already predicted a red-shifted or normal N—H···F H-bond in the same complex at B3LYP/6-31+G(d,p), B3LYP/6-311+G(d,p) and B3LYP/6-311++G(3df, 3pd) levels. Both MP2 and B3LYP computations have their own supporting instances from the point of agreement between theoretical prediction and experimental measurement.[2,16] Consequently, it is difficult to decide which H-bond type of N—H···F in $NHF_2\cdots HF$ complex takes from the theoretical point of view. As a result, it is not yet known whether blue-shifted H-bonds can be observed in N—H···Y system. To the best of our knowledge, the largest calculated blue shift in the vibrational frequency for X—H···Y H-bond is close to 60 cm^{-1}.[9] From a purely theoretical viewpoint, the upper limit for a blue shift is an interesting question. Our main goal of this article is to find cases where N—H bond exhibits a substantial blue shift in the vibrational frequency while the hyperconjugative $n(O)\rightarrow\sigma^*(N—H)$ interaction is quite strong. Our results show that the blue shifted N—H stretching frequency of 120 cm^{-1} calculated is the largest ever reported in the literature. Furthermore, a reasonable explanation for the origin of the blue-shifted H-bond was proposed.

Computational methods

The structures and vibrational frequencies of the $HNO\cdots H_2O_2$ complex were investigated using both standard and counterpoise-corrected (CP) optimization methods at MP2/6-31G(d), MP2/6-31+G(d,p), MP2/6-311++G(d,p), B3LYP/6-31G(d), B3LYP/6-31+G(d,p) and B3LYP/6-311++G(d,p) levels, respectively.[33,34] The basis set superposition errors (BSSE) were calculated according to the counterpoise method proposed by Boys and Bernardi.[34] Analyses of natural bond orbital (NBO)[35] and atoms in molecules (AIM)[36] were both carried out at MP2/6-31+G(d,p) level. All the calculations were performed via the Gaussian 03 program packages.[37]

* E-mail: yongyang@aiofm.ac.cn
Received August 22, 2005; revised December 9, 2005; accepted March 22, 2006.
Project supported by the National Natural Science Foundation of China (No. G20477043) and Knowledge Creative Program of Chinese Academy of Sciences (No. KJCX2-SW-H08).

Results and discussion

Geometries, frequencies and energies

The characteristics of HNO···H_2O_2 complex determined by both standard and CP optimization procedures, are presented in Tables 1, 2 and Figure 1. From N(2)—H(1) stretching frequency change between the monomer HNO and the complex HNO···H_2O_2 shown in Tables 1 and 2, we can see that there is a small difference between MP2 and B3LYP calculations. For example, the MP2/6-311 + + G(d,p) computation predicted that N(2)—H(1) stretching frequency of the monomer HNO and the complex HNO···H_2O_2 were 3027 and 3151 cm^{-1}, respectively, which implies 124 cm^{-1} blue shift of the N—H stretching frequency. The B3LYP/6-311++G(d,p) computation predicted 139 cm^{-1} blue shift of the N—H stretching frequency with those of the monomer and the complex to be 2862 and 3001 cm^{-1}, respectively. As far as the H-bond type prediction was concerned, the MP2 computation results were in good agreement with those of the B3LYP, indicating that the N(2)—H(1) stretching frequency has a very large blue shift in HNO···H_2O_2 complex. On the contrary, we can see that there is a disagreement between MP2 and B3LYP calculations in predicting H-bond type of NHF_2···HF complex.[7,23,28] Obviously, it is very dangerous to identify H-bond type by theoretical calculations when the X—H bond length change is very small in X—H···Y H-bond. The contradictory H-bond type prediction between MP2 and B3LYP calculations can only be resolved with the aid of experimental infrared spectrum measurement. To evaluate the influence of basis sets, the N(2)—H(1) stretching frequency change was calculated by both MP2 and B3LYP methods with 6-31G(d), 6-31+G(d,p) and 6-311++G(d,p) basis sets, respectively. Table 1 shows that the MP2/6-31+G(d,p) and MP2/6-311++G(d,p) values of the N(2)—H(1) stretching frequency change are in excellent agreement, while the corresponding MP2/6-31G(d) values are larger in magnitude. It seems that the larger the basis set, the less the difference of the stretching frequency change. Influence of basis sets was also investigated for B3LYP calculation, and similar results were obtained. Taking the $(HF)_2$ complex as an example, the necessity to use the CP-corrected gradient optimization was pointed out by Hobza *et al.*[38] The CP-corrected gradient optimization will affect not only the interaction energy but also the geometry and stretching frequency of the X—H···Y H-bond. However, the large blue shift of the N(2)—H(1) stretching frequency in HNO···H_2O_2 complex by both MP2 and B3LYP calculation still exists, as shown also in Tables 1 and 2, in spite of application of the CP-corrected. On the other hand, the blue shift of the N(2)—H(1) stretching frequency by CP-corrected optimization is slightly smaller but still in reasonable agreement with this of the N(2)—H(1) stretching frequency by standard optimization. On the basis of these analyses, the N(2)—H(1) stretching frequency can be confirmed to display a very large blue shift (about 120 cm^{-1}). In addition, there exists another O(5)—H(4)··· O(3) H-bond in HNO···H_2O_2 complex. As shown in Tables 1 and 2, the O(5)—H(4) bond exhibits characteristic features of the classical H-bond, *i.e.*, elongation of O(5)—H(4) bond and the red shift of its stretching frequency.

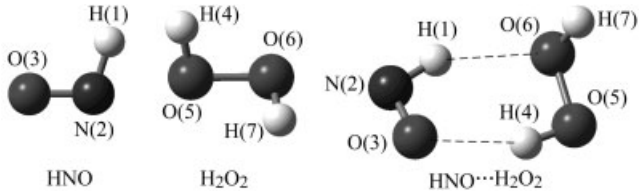

Figure 1 Optimized structures of HNO, H_2O_2 and HNO···H_2O_2 complex.

Table 1 Characteristics of HNO···H_2O_2 complex with different (standard and CP-corrected) optimization at MP2/6-31G(d), MP2/6-31+G(d,p) and MP2/6-311++G(d,p) levels

	MP2/6-31G(d)		MP2/6-31+G(d,p)		MP2/6-311++G(d,p)	
	Standard	CP	Standard	CP	Standard	CP
r[O(3)···H(4)]/nm	0.20119	0.20871	0.20378	0.21179	0.20529	0.21533
r[O(6)···H(1)]/nm	0.21789	0.22628	0.22191	0.23027	0.22477	0.23273
Δr^a[N(2)—H(1)]/nm	−0.00087	−0.00071	−0.00058	−0.00054	−0.00067	−0.00061
$\Delta\nu^b$[N(2)—H(1)]/cm^{-1}	+155	+130	+116	+107	+124	+112
Δr[O(5)—H(4)]/nm	+0.00052	+0.00046	+0.00053	+0.00043	+0.00047	+0.00038
$\Delta\nu$[O(5)—H(4)]/cm^{-1}	−71	−65	−90	−77	−83	−61
ΔE^c/(kJ•mol^{-1})	−33.39	−32.72	−28.20	−27.78	−25.44	−24.98
ΔE(CP)^d/(kJ•mol^{-1})	−20.50	−21.17	−20.33	−20.79	−18.62	−19.12
ΔE(CP, ZPE)^e/(kJ•mol^{-1})	−10.59	−12.47	−11.67	−12.89	−10.63	−11.51

[a] Change of bond length. [b] Change of stretching frequency. [c] Intermolecular interaction energy. [d] Intermolecular interaction energy with BSSE correction. [e] Intermolecular interaction energy with both BSSE correction and ZPE correction.

Table 2 Characteristics of HNO···H_2O_2 complex with different (standard and CP-corrected) optimization at B3LYP/6-31G(d), B3LYP/6-31+G(d,p) and B3LYP/6-311++G(d,p) levels

	B3LYP/6-31G(d)		B3LYP/6-31+G(d,p)		B3LYP/6-311++G(d,p)	
	Standard	CP	Standard	CP	Standard	CP
r[O(3)···H(4)]/nm	0.19743	0.20140	0.20193	0.20465	0.20243	0.20574
r[O(6)···H(1)]/nm	0.21381	0.21857	0.22073	0.22480	0.22186	0.22550
Δr^a[N(2)—H(1)]/nm	−0.00119	−0.00103	−0.00073	−0.00071	−0.00082	−0.00078
$\Delta\nu^b$[N(2)—H(1)]/cm^{-1}	+180	+161	+131	+127	+139	+132
Δr[O(5)—H(4)]/nm	+0.00069	+0.00065	+0.00072	+0.00066	+0.00069	+0.00063
$\Delta\nu$[O(5)—H(4)]/cm^{-1}	−107	−105	−124	−115	−122	−111
ΔE^c/(kJ•mol^{-1})	−33.01	−32.59	−24.23	−24.14	−23.72	−23.64
ΔE(CP)^d/(kJ•mol^{-1})	−21.88	−22.18	−21.13	−21.21	−21.09	−21.17
ΔE(CP, ZPE)^e/(kJ•mol^{-1})	−11.72	−12.80	−12.47	−12.84	−12.51	−12.80

[a] Change of bond length. [b] Change of stretching frequency. [c] Intermolecular interaction energy. [d] Intermolecular interaction energy with BSSE correction. [e] Intermolecular interaction energy with both BSSE correction and ZPE correction.

As shown in Tables 1 and 2, the intermolecular interaction energies with both BSSE correction and ZPE correction are in reasonable agreement at various levels. In addition, the results indicate that BSSE correction and ZPE correction are important to accurately describe the intermolecular interaction energies.

AIM topological analysis

To confirm the existence of the H-bonds in HNO··· H_2O_2 complex, AIM topological analysis was performed. Popelier *et al.*[39,40] proposed a set of criteria for the existence of H-bonds, among which three were most often applied.[41] The electron density and its Laplacian for H···Y contact within the X—H···Y H-bond should have a relatively high value. Both parameters for closed-shell interactions as H-bond are positive and should be within the following ranges: 0.002—0.035 for the electron density and 0.024—0.139 for its Laplacian. According to the topological analysis of electron density in the theory of AIM, ρ was used to describe the strength of a bond. In general, the larger the value of ρ is, the stronger the bond is. The $\bigtriangledown^2\rho$ describes the characteristic of the bond, where $\bigtriangledown^2\rho<0$, the bond is covalent bond, as $\bigtriangledown^2\rho>0$, the bond belongs to the ionic bond, hydrogen bond or van der Waals interaction.[42] Here, $\bigtriangledown^2\rho=\lambda_1+\lambda_2+\lambda_3$, and λ_i is an eigenvalue of the Hessian matrix of ρ. Then, when one of the three λ_i was positive and the other two were negative, it was denoted by (3, −1) and called the bond critical point (BCP). When one of the three λ_i was negative and the other two were positive, it was denoted by (3, +1) and called the ring critical point (RCP), indicating that a ring structure exists. As shown in Table 3, the values of the electron density ρ for O(6)···H(1) and O(3)···H(4) in HNO··· H_2O_2 complex are 0.01475 and 0.01953, respectively. These values did fall within the proposed typical range of H-bonds. Since ρ[O(6)···H(1)] was smaller than ρ[O(3)···H(4)] in HNO···H_2O_2 complex, the former bond was expected to be weaker than the latter. The values of the $\bigtriangledown^2\rho$ for O(6)···H(1) and O(3)···H(4) are 0.04873 and 0.06333, respectively, and such values are also in the range of the H-bonds. In addition, it is worthy of mentioning that there is an RCP in HNO···H_2O_2 complex, indicating the existence of six-membered ring of H(1)-N(2)-O(3)-H(4)-O(5)-O(6).

On the basis of the AIM topological analysis, it was proved that the N(2)—H(1)···O(6) and O(5)—H(4)··· O(3) bonds can be classified as H-bonds in HNO··· H_2O_2 complex. It should be pointed out that N(2)—H(1) bond exhibits a large blue shift whereas O(5)—H(4) bond exhibits a red shift. However, the AIM analysis did not reveal the origin of the red-shifted and blue-shifted H-bonds, and this problem was solved by the NBO analysis.

Table 3 Topological parameters of the bond critical point and ring critical point in HNO···H_2O_2 complex at MP2/6-31+G(d,p) level

	ρ	$\bigtriangledown^2\rho$	λ_1	λ_2	λ_3
BCP					
O(6)···H(1)	0.01475	0.04873	0.01792	−0.01644	0.08309
O(3)···H(4)	0.01953	0.06333	−0.02585	−0.02429	0.11350
RCP					
H(1)—N(2)—O(3)—H(4)—O(5)—O(6)	0.00744	0.03969	−0.00586	0.00811	0.03744

NBO analysis

It is clear from Figure 1 that the H-bonds are complicated in HNO···H_2O_2 complex, which exhibits simultaneously the red-shifted O(5)—H(4)···O(3) and blue-shifted N(2)—H(1)···O(6) H-bonds. To interpret the origins of the red-shifted and blue-shifted H-bonds in HNO···H_2O_2 complex, the NBO analysis was performed and the corresponding results are presented in Table 4. In the NBO analysis, the importance of hyperconjugative interaction and electron density transfer from lone electron pairs of the Y atom to the X—H antibonding orbital in the X—H···Y system was well-documented.[35] In general, such interaction leads to an increase in population of X—H antibonding orbital. The increase of electron density in X—H antibonding orbital weakens the X—H bond, which leads to its elongation and concomitant red shift of the X—H stretching frequency. Furthermore, Alabugin *et al.*[26] have recently shown that structural reorganization of X—H bond in the process of both blue-shifted and red-shifted H-bonds was determined by the balance of the opposing effects: X—H bond lengthening effect due to hyperconjugative n(Y)→σ^*(X—H) interaction and X—H bond shortening effect due to rehybridization, and also suggested that red shift and blue shift should be determined by the threshold to correspond to the hyperconjugative n(Y)→σ^*(X—H) interaction in the order of 13—21 kJ/mol. The red-shifted H-bond was observed when the X—H bond lengthening hyperconjugative n(Y)→σ^*(X—H) interaction was relatively strong (NBO energy value for this interaction was larger than 21 kJ/mol). The blue-shifted H-bond was likely to be observed only when the X—H bond lengthening hyperconjugative n(Y)→σ^*(X—H) interaction was relatively weak (NBO energy value for this interaction was less than 13 kJ/mol). On the basis of the theoretical model, it should not be difficult to explain the red shift of O(5)—H(4) stretching frequency in HNO···H_2O_2 complex. For O(5)—H(4)··· O(3) H-bond, Table 4 shows that O(5)—H(4) bond lengthening hyperconjugative n[O(3)]→σ^*[O(5)—H(4)] interaction was relatively strong (NBO energy value for this interaction was larger than 21 kJ/mol threshold), which indicates the dominant role of hyperconjugation. The corresponding increase of electron density in σ^*[O(5)—H(4)] was able to weaken and elongate the O(5)—H(4) bond, which results in the red shift of the O(5)—H(4) stretching frequency. On the other hand, according to the rehybridization model, the O(5)—H(4)···O(3) H-bond formation increased the O(5)—H(4) bond polarization and positive charge on H(4) atom.

Table 4 NBO analysis of HNO, H_2O_2 and HNO···H_2O_2 at MP2/6-31+G(d,p) level

	HNO	H_2O_2	HNO···H_2O_2
$\Delta E^{(2)a}n_1$[O(6)]→σ^*[N(2)—H(1)]/(kJ•mol^{-1})	—	—	0.67
$\Delta E^{(2)}n_2$[O(6)]→σ^*[N(2)—H(1)]/(kJ•mol^{-1})	—	—	21.55
$\Delta E^{(2)}n_1$[O(3)]→σ^*[O(5)—H(4)]/(kJ•mol^{-1})	—	—	16.48
$\Delta E^{(2)}n_2$[O(3)]→σ^*[O(5)—H(4)]/(kJ•mol^{-1})	—	—	26.23
$\Delta E^{(2)}n_1$[O(3)]→σ^*[N(2)—H(1)]/(kJ•mol^{-1})	—	—	6.78
$\Delta E^{(2)}n_2$[O(3)]→σ^*[N(2)—H(1)]/(kJ•mol^{-1})	61.21	—	43.47
$\Delta E^{(2)}n_2$[O(6)]→σ^*[O(5)—H(4)]/(kJ•mol^{-1})	—	4.14	3.89
E-index[N(2)—H(1)···O(6)]	—	—	0.49
E-index[O(5)—H(4)···O(3)]	—	—	0.01
σ^*[N(2)—H(1)]/e	0.02462	—	0.02645
$\Delta\sigma^{*\,b}$[N(2)—H(1)]/e	—	—	0.00183
σ^*[O(5)—H(4)]/e	—	0.00260	0.01616
$\Delta\sigma^*$[O(5)—H(4)]/e	—	—	0.01356
q[H(1)]/e	0.32756	—	0.35693
sp^n[N(2)—H(1)]	sp$^{3.52}$	—	sp$^{3.15}$
s-char^c/%	22.10	—	24.03
pol[N(2)]^d/%	67.23	—	68.81
[$\sigma_{N(2)-H(1)}$], H(1)/%	32.77	—	31.19
q[H(4)]	—	0.50736	0.52518
sp^n[O(5)—H(4)]	—	sp$^{3.20}$	sp$^{2.76}$
s-char/%	—	23.80	26.53
Pol[O(5)]/%	—	75.57	77.05
[$\sigma_{O(5)-H(4)}$], H(4)/%	—	24.43	22.95

[a] Energy of hyperconjugative interaction. [b] Change in the occupation of σ^* orbital. [c] s-character in the hybrid orbital. [d] Bond polarization.

These changes resulted in a simultaneous increase in the s-character in the O(5) hybrid orbital of O(5)—H(4) bond, which should lead to O(5)—H(4) bond contraction. Table 4 shows that the s-character of O(5)—H(4) bond in O(5)—H(4)···O(3) H-bond was increased from $sp^{3.20}$ to $sp^{2.76}$, which strengthens the O(5)—H(4) bond. Because hyperconjugation and rehybridization act in opposite directions, the red shift and blue shift of the bond X—H is a result of a balance of two effects. Then, the fact is simple: the hyperconjugation is dominant and overshadows the rehybridization in O(5)—H(4)···O(3) H-bond. To this point, the NBO results can fully explain the observations of the red shift of the O(5)—H(4) stretching frequency in HNO···H_2O_2 complex.

More attention was paid to the change of the N(2)—H(1) stretching frequency in HNO···H_2O_2 complex. It is worth pointing out that the change of N(2)—H(1) stretching frequency has an evident difference from that of O(5)—H(4) stretching frequency in HNO···H_2O_2 complex. As shown in Table 4, the hyperconjugative n[O(6)]→σ*[N(2)—H(1)] interaction is slightly above 21 kJ/mol threshold, indicating that the hyperconjugation will play a dominant role. However, it is surprising that the very large blue shift of N(2)—H(1) stretching frequency was in fact observed in Tables 1 and 2. The question is how to explain so large a blue shift of N(2)—H(1) stretching frequency. First, the electron density redistribution was noted to play a significant role. In the type of Z—X—H···Y H-bond, where Z is an electronegative atom having one or more lone electron pairs (such as F, O, N), the hyperconjugative n(Y)→σ*(X—H) interaction leads to an increase of electron density in σ*(X—H). On the other hand, a decrease in the n(Z)→σ*(X—H) interaction of the complex, relative to the monomer, has the opposite effect. As a result, the net change of electron density in σ*(X—H) and the ultimate direction of the X—H bond length change depend on the balance of these two interactions which changed in an antiparallel way. It may be of interest to make a quantitative comparison between these two interactions. Then, a novel index was defined and called *E*-index, which can be determined as a ratio of the variable magnitude of the n(Z)→σ*(X—H) interaction to the magnitude of the n(Y)→σ*(X—H) interaction in the Z—X—H···Y system. Here, the *E*-index can be expressed as

$$E\text{-index} = \frac{E_{\text{monomer}}[\text{n(Z)}\rightarrow\sigma^*(\text{X—H})] - E_{\text{complex}}[\text{n(Z)}\rightarrow\sigma^*(\text{X—H})]}{E[\text{n(Y)}\rightarrow\sigma^*(\text{X—H})]} \quad (1)$$

where E_{monomer}[n(Z)→σ*(X—H)] and E_{complex} [n(Z)→σ*(X—H)] mean the n(Z)→σ*(X—H) interactions in the monomer and complex, respectively, while *E*[n(Y)→σ*(X—H)] denotes the n(Y)→σ*(X—H) interaction in the complex. According to the definition of the *E*-index, the *E*-index can be used to describe the strength of the electron density redistribution. In general, the larger the value of *E*-index is, the stronger the electron density redistribution effect. As shown in Table 4, the magnitude of n[O(3)]→σ*[N(2)—H(1)] interactions has an evident change of monomer HNO with respect to that of HNO···H_2O_2 complex. The interaction is stronger in the monomer HNO than in HNO···H_2O_2 complex. Furthermore, the value of the *E*-index [N(2)—H(1)···O(6)] is relatively large and attains 0.49, indicating that the electron density redistribution effect is very significant in the N(2)—H(1)···O(6) H-bond. As a result, it can be seen that the net increase of electron density in σ*[N(2)—H(1)] is quite small in HNO···H_2O_2 complex, relative to that in the monomer HNO. A part transfer of the electron density was suggested from the lone electron pairs of O(6) atom in H_2O_2 to the lone electron pairs of O(3) atom in HNO instead of the N(2)—H(1) antibonding orbital through electron density redistribution. Consequently, the N(2)—H(1) bond lengthening effect of hyperconjugation can be believably inhibited greatly due to the existence of electron density redistribution effect. On the other hand, it is worthy of mentioning that the rehybridization effect is very strong for the N(2)—H(1) bonds. Table 4 shows the s-character increase of the sp^n hybrid orbitals from $sp^{3.52}$ to $sp^{3.15}$ for N(2)—H(1). The very large increase of s-character results in the intense contraction of the N(2)—H(1) bond. On the basis of these analyses, there can be conclusively two effects to decrease the N(2)—H(1) bond length and lead to a blue shift of the N(2)—H(1) stretching frequency. The first effect is connected with the electron density redistribution in the N(2)—H(1)···O(6) H-bond, and the second effect is connected with the rehybridization of sp^n N(2)—H(1) hybrid orbital. According to such analyses, the surprising large blue shift of N(2)—H(1) stretching frequency can well be explained. Because the N(2)—H(1) bond lengthening effect of hyperconjugation is greatly inhibited, the N(2)—H(1) bond shortening effect of rehybridization can be expectantly dominant to overcome the N(2)—H(1) bond lengthening effect of hyperconjugation. The situation in O(5)—H(4)···O(3) H-bond was noted to be different from N(2)—H(1)···O(6) H-bond. The value of *E*-index [O(5)—H(4)···O(3)] is very small, indicating that the electron density redistribution effect is very weak in O(5)—H(4)···O(3) H-bond. The dominant part of the electron density transfer from the lone electron pairs of O(3) atom in HNO is directed to the O(5)—H(4) antibonding orbital. The corresponding large increase of electron density in σ*[O(5)—H(4)] causes weakening of O(5)—H(4) bond.

In summary, the calculations show that the complex HNO···H_2O_2 exhibits simultaneously O(5)—H(4)···O(3) red-shifted and N(2)—H(1)···O(6) blue-shifted H-bonds. For the O(5)—H(4)···O(3) red-shifted H-bond, the hyperconjugation is relatively strong and the electron density redistribution is not significant. Then, the O(5)—

H(4)···O(3) red-shifted H-bond can be easily explained on the basis of hyperconjugation and rehybridization. For the N(2)—H(1)···O(6) blue-shifted H-bond, the electron density redistribution was believed to be an important effect to explain the lager blue shift of N(2)—H(1) stretching frequency. The N(2)—H(1) bond lengthening effect of hyperconjugation is greatly inhibited due to the existence of significant electron density redistribution effect. Hence, the large blue shift of the N(2)—H(1) stretching frequency appears because the rehybridization overcomes the hyperconjugation.

Conclusion

The complex HNO···H_2O_2 has been investigated with both standard and counterpoise-corrected optimization methods at MP2/6-31G(d), MP2/6-31+G(d,p), MP2/6-311++G(d,p), B3LYP/6-31G(d), B3L-YP/6-31+G(d,p) and B3LYP/6-311++G(d,p) levels, respectively. The complex HNO···H_2O_2 exhibits simultaneously O(5)—H(4)···O(3) red-shifted and N(2)—H(1)···O(6) blue-shifted H-bonds. The calculations show that the N(2)—H(1) stretching frequency displays a very large blue shift (about 120 cm^{-1}). This value of blue shift is the largest for X—H···Y H-bonds as reported in the literature so far. From the NBO analysis, it became evident that the O(5)—H(4)···O(3) red-shifted H-bond can be evidently explained on the basis of the fact that the bond lengthening effect of hyperconjugation overcame the bond shortening effect of rehybridization. For the N(2)—H(1)···O(6) blue-shifted H-bond, the N(2)—H(1) bond lengthening effect of hyperconjugation was greatly inhibited due to the significant electron density redistribution effect. Consequently, N(2)—H(1) bond shortening effect was dominant, which can lead to a large blue shift of N(2)—H(1) stretching frequency.

References

1 Delanoye, S. N.; Herrebout, W. A.; van der Veken, B. J. *J. Am. Chem. Soc.* **2002**, *124*, 11854.
2 Hobza, P.; Špirko, V.; Havlas, Z.; Buchhold, K.; Reimann, B.; Barth, H. D.; Brutschy, B. *Chem. Phys. Lett.* **1999**, *299*, 180.
3 Reimann, B.; Buchhold, K.; Vaupel, S.; Brutschy, B.; Havlas, Z.; Špirko, V.; Hobza, P. *J. Phys. Chem. A* **2001**, *105*, 5560.
4 Hobza, P.; Špirko, V.; Selzle, H. L.; Schlag, E. W. *J. Phys. Chem. A* **1998**, *102*, 2501.
5 Chocholoušová, J.; Špirko, V.; Hobza, P. *Phys. Chem. Chem. Phys.* **2004**, *6*, 37.
6 Mrázková, E.; Hobza, P. *J. Phys. Chem. A* **2003**, *107*, 1032.
7 Hobza, P. *Int. J. Quantum Chem.* **2002**, *90*, 1071.
8 Hobza, P.; Havlas, Z. *Chem. Rev.* **2000**, *100*, 4253.
9 Karpfen, A.; Kryachko, E. S. *J. Phys. Chem. A* **2003**, *107*, 9724.
10 Kryachko, E. S.; Zeegers-Huyskens, T. *J. Phys. Chem. A* **2001**, *105*, 7118.
11 Kryachko, E. S.; Zeegers-Huyskens, T. *J. Phys. Chem. A* **2003**, *107*, 7546.
12 McDowell, S. A. *J. Chem. Phys.* **2003**, *119*, 3711.
13 McDowell, S. A. *J. Chem. Phys.* **2003**, *118*, 7283.
14 McDowell, S. A. *Phys. Chem. Chem. Phys.* **2003**, *5*, 808.
15 McDowell, S. A. *J. Mol. Struct.* (*Theochem*) **2003**, *625*, 243.
16 Matsuura, H.; Yoshida, H.; Hieda, M.; Yamannaka, S.; Harada, T.; Shin-ya, K.; Ohno, K. *J. Am. Chem. Soc.* **2003**, *125*, 13910.
17 Yoshida, H.; Harada, T.; Murase, T.; Ohno, K.; Matsuura, H. *J. Phys. Chem. A* **1997**, *101*, 1731.
18 Harada, T.; Yoshida, H.; Ohno, K.; Matsuura, H. *Chem. Phys. Lett.* **2002**, *362*, 453.
19 Gu, Y.; Kar, T.; Scheiner, S. *J. Am. Chem. Soc.* **1999**, *121*, 9411.
20 Scheiner, S.; Grabowski, S. J.; Kar, T. *J. Phys. Chem. A* **2001**, *105*, 10607.
21 Scheiner, S.; Kar, T. *J. Phys. Chem. A* **2002**, *104*, 9428.
22 Fang, Y.; Fan, J. M.; Liu, L.; Li, X. S.; Guo, Q. X. *Chem. Lett.* **2002**, *31*, 116.
23 Li, X. S.; Liu, L.; Scheiner, H. B. *J. Am. Chem. Soc.* **2002**, *124*, 9636.
24 Hermansson, K. *J. Phys. Chem. A* **2002**, *106*, 4695.
25 Masunov, A.; Dannenberg, J. J.; Contreras, R. *J. Phys. Chem. A* **2001**, *105*, 4737.
26 Alabugin, I. V.; Manoharan, M.; Peabody, S.; Weinhold, F. *J. Am. Chem. Soc.* **2003**, *125*, 5973.
27 Alabugin, I. V.; Manoharan, M.; Weinhold, F. *J. Phys. Chem. A* **2004**, *108*, 4270.
28 Lu, P.; Liu, G. Q.; Li, J. C. *J. Mol. Struct.* (*Theochem*) **2005**, *723*, 95.
29 Shi, F. Q.; An, J. Y.; Li, W.; Zhao, S.; Yu, J. Y. *Acta Chim. Sinica* **2004**, *62*, 1171 (in Chinese).
30 Li, J.; Xie, D. Q.; Yan, G. S. *Sci. China, Ser. B* **2003**, *33*, 21 (in Chinese).
31 Wang, X.; Zhou, G.; Tian, A. M.; Wong, N. B. *J. Mol. Struct.* (*Theochem*) **2005**, *718*, 1.
32 Yang, Y.; Zhang, W. J.; Pei, S. X.; Shao, J.; Huang, W.; Gao, X. M. *J. Mol. Struct.* (*Theochem*) **2005**, *732*, 33.
33 Simon, S.; Duran, M.; Dannenbery, J. J. *J. Chem. Phys.* **1996**, *105*, 11024.
34 Boys, S. F.; Bernardi, F. *Mol. Phys.* **1970**, *19*, 553.
35 Reed, A. E.; Curtiss, L. A.; Weinhold, F. *Chem. Rev.* **1988**, *88*, 899.
36 Bader, R. F. W. *Atoms in Molecules*: *A Quantum Theory*, Oxford University Press, Oxford, **1990**.
37 Frisch, M. J.; Trucks, G. W.; Schlegel, H. B.; Scuseria, G. E.; Robb, M. A.; Cheeseman, J. R.; Montgomery, J. A. Jr.; Vreven, T.; Kudin, K. N.; Burant, J. C.; Millam, J. M.; Iyengar, S. S.; Tomasi, J.; Barone, V.; Mennucci, B.; Cossi, M.; Scalmani, G.; Rega, N.; Petersson, G. A.; Nakatsuji, H.; Hada, M.; Ehara, M.; Toyota, K.; Fukuda, R.; Hasegawa, J.; Ishida, M.; Nakajima, T.; Honda, Y.; Kitao, O.; Nakai, H.; Klene, M.; Li, X.; Knox, J. E.; Hratchian, H. P.; Cross, J. B.; Adamo, C.; Jaramillo, J.; Gomperts, R.; Stratmann, R. E.; Yazyev, O.; Austin, A. J.; Cammi, R.; Pomelli, C.; Ochterski, J. W.; Ayala, P. Y.; Morokuma, K.; Voth, G. A.; Sal-

vador, P.; Dannenberg, J. J.; Zakrzewski, V. G.; Dapprich, S.; Daniels, A. D.; Strain, M. C.; Farkas, O.; Malick, D. K.; Rabuck, A. D.; Raghavachari, K.; Foresman, J. B.; Ortiz, J. V.; Cui, Q.; Baboul, A. G.; Clifford, S.; Cioslowski, J.; Stefanov, B. B.; Liu, G.; Liashenko, A.; Piskorz, P.; Komaromi, I.; Martin, R. L.; Fox, D. J.; Keith, T.; Al-Laham, M. A.; Peng, C. Y.; Nanayakkara, A.; Challacombe, M.; Gill, P. M. W.; Johnson, B.; Chen, W.; Wong, M. W.; Gonzalez, C.; Pople, J. A. *Gaussian 03*, Revision B. 02, Gaussian, Inc., Pittsburgh PA, **2003**.

38 Hobza, P.; Halvas, Z. *Theor*. *Chim*. *Acta* **1988**, *99*, 372.

39 Kock, U.; Popelier, P. L. A. *J*. *Phys*. *Chem*. **1995**, *99*, 9747.

40 Popelier, P. L. A. *J*. *Phys*. *Chem*. *A* **1998**, *102*, 1873.

41 Lipkowski, P.; Grabowski, S. J.; Robinson, T. L.; Leszczynski, J. *J*. *Phys*. *Chem*. *A* **2004**, *108*, 10865.

42 Zeng, Y. L.; Zheng, S. J.; Meng, L. P.; Wang, D. X. *Acta Chim*. *Sinica* **2004**, *62*, 1101 (in Chinese).

(E0508222 SONG, J. P.)